

# Nonpartonic components in the nucleon structure functions at small $Q^2$ in a broad range of $x$

A. Szczurek<sup>1</sup>, V. Uleshchenko<sup>1,2</sup>

<sup>1</sup> Institute of Nuclear Physics, 31-342 Cracow, Poland

<sup>2</sup> Institute for Nuclear Research, 252028 Kiev, Ukraine

Received: 10 May 1999 / Revised version: 9 July 1999 /  
Published online: 3 February 2000 – © Springer-Verlag 2000

**Abstract.** We construct a simple two-phase model of the nucleon structure functions valid for both small and large  $Q^2$  and in the broad range of Bjorken  $x$ . The model incorporates hadron dominance at small  $x$  and  $Q^2$  and parton model at large  $Q^2$ . The VDM contribution is modified for small fluctuation times of the hadronic state of the photon. With two free parameters we describe SLAC, CERN NMC, Fermilab E665 and CERN BCDMS data for both proton and deuteron structure functions. Our model explains some phenomenological higher-twist effects extracted from earlier analyses. A good description of the NMC  $F_2^p(x) - F_2^n(x)$  data is obtained in contrast to other models in the literature. We predict faster vanishing of the partonic component at low  $Q^2$  than previously expected and strong  $Q^2$  dependence of the Gottfried Sum Rule below  $Q^2 \approx 4 \text{ GeV}^2$ .

## 1 Introduction

The standard deep inelastic scattering picture applies when the four-momentum transfer squared from the lepton line to the hadron line ( $Q^2$ ) is large. When virtual photon wave length increases and reaches the size of the nucleon one may expect a transition to another regime where the standard partonic model is no longer valid. In this region a kinematical constraint [1] guarantees the vanishing of the  $F_2(x, Q^2)$  structure function. This requirement is not embodied in the perturbative parton distributions. A phenomenological fit based on parton screening was proposed in [2] to satisfy this condition by introducing an extra form factor.

The recent low- $Q^2$  data from HERA [3,4] have triggered many phenomenological analyses. Especially interesting is the unexplored transition region. At present there is no consensus on the details of the transition mechanism. Here we concentrate on the region of somewhat larger  $x$  rather than the new HERA data. We shall demonstrate that also at larger  $x$  a similar transition due to vanishing partonic components at small  $Q^2$  takes place, although it is not directly seen from experimental data.

It is common wisdom that the vector dominance model applies at low  $Q^2$  while the parton model describes the region of large  $Q^2$ , leading at lowest order to Bjorken scaling, and to logarithmic scaling violation in higher orders of QCD. A proposal was made in [7] to unify both the limits in a consistent dispersion method approach. In the traditional formulation of the VDM one is limited to large lifetimes of hadronic fluctuations of the virtual photon, i.e. small Bjorken  $x < 0.1$  for the existing data. It is a purpose

of this paper to generalize the model to a full range of  $Q^2$  and  $x$  by introducing extra phenomenological form factors to be adjusted to the experimental data.

Some authors believe that it is old-fashioned to talk about VDM contribution in the QCD era. However, VDM effects appear naturally in the time-like region in the production of vector mesons in  $e^+e^-$  collisions. These effects cannot be described in terms of perturbative QCD, as in the production of resonances many complicated nonperturbative effects take place. The physics must be similar in the space-like region. We shall demonstrate that it is essential to include this contribution explicitly in order to describe the structure functions at low  $Q^2$ .

In the next section we outline our model and discuss how to choose its basic parameters in a model independent way. In Sect. 3 we discuss a fit of the remaining parameters to the fixed target data and present results of the fitting procedure for the proton and deuteron structure functions. In addition we compare the result of our model for  $F_2^p - F_2^n$  and some subtle isovector higher-twist effects with another low- $Q^2$  model. Finally we discuss some interesting predictions which could be verified in the future.

## 2 The model

As in [7] the total nucleon structure function is represented as a sum of the standard vector dominance part, important at small  $Q^2$  and/or small Bjorken  $x$ , and partonic (*part*) piece which dominates over the vector dominance

(VDM) part at large  $Q^2$ :

$$F_2^N(x, Q^2) = F_2^{N,VDM}(x, Q^2) + F_2^{N,part}(x, Q^2). \quad (1)$$

The standard range of applicability of vector dominance contribution is limited to large invariant masses of the hadronic system ( $W$ ), i.e. small values of  $x$ . In the target (nucleon) reference frame the time of life of the hadronic fluctuation is given according to the uncertainty principle as  $\tau \sim 1/\Delta E$  with

$$\Delta E = \sqrt{M_V^2 + |\mathbf{q}|^2} - \sqrt{q^2 + |\mathbf{q}|^2}, \quad (2)$$

where  $M_V$  is the mass of the hadronic fluctuation (vector meson mass). In terms of the photon virtuality and Bjorken  $x$  this can be expressed as

$$\Delta E = \frac{M_V^2 + Q^2}{Q^2} \cdot M_N x. \quad (3)$$

As the energy transfer  $\nu \rightarrow \infty$  the time of life of the hadronic fluctuation becomes  $\tau \sim \frac{Q^2}{M_V^2 m_N x}$ . It is natural to expect small VDM contribution when the time of life of the hadronic fluctuation is small. We shall model this fact by introducing a form factor  $\Omega(\tau) = \Omega(x, Q^2)$ . Then the modified vector dominance contribution can be written as:

$$F_2^{N,VDM}(x, Q^2) = \frac{Q^2}{\pi} \sum_V \frac{M_V^4 \cdot \sigma_{VN}^{tot}(s^{1/2})}{\gamma_V^2 (Q^2 + M_V^2)^2} \cdot \Omega_V(x, Q^2). \quad (4)$$

In the present paper we take  $\gamma$ 's calculated from the leptonic decays of vector mesons which include finite width corrections [8]  $\gamma_\rho^2/4\pi = 2.54$ ,  $\gamma_\omega^2/4\pi = 20.5$ ,  $\gamma_\phi^2/4\pi = 11.7$ .<sup>1</sup>

In general one can try different functional forms for  $\Omega$ . In the present analysis we shall use only exponential and Gaussian form factors

$$\begin{aligned} \Omega(x, Q^2) &= \exp(-\Delta E/\lambda_E), \\ \Omega(x, Q^2) &= \exp(-(\Delta E/\lambda_G)^2). \end{aligned} \quad (5)$$

As in [7] we take the partonic contribution as

$$F_2^{N,part}(x, Q^2) = \frac{Q^2}{Q^2 + Q_0^2} \cdot F_2^{asympt}(\bar{x}, \bar{Q}^2). \quad (6)$$

where  $\bar{x} = \frac{Q^2 + Q_2^2}{W^2 - m_N^2 + Q^2 + Q_2^2}$  and  $\bar{Q}^2 = Q^2 + Q_1^2$ . The  $F_2^{asympt}(x, Q^2)$  above denotes the standard partonic structure function which in the leading order can be expressed in terms of the quark distributions:

$$F_2^{asympt}(x, Q^2) = x \cdot \sum_f e_f^2 \cdot [q_f(x, Q^2) + \bar{q}_f(x, Q^2)].$$

The extra factor in front of (6) assures a correct kinematic behaviour in the limit  $Q^2 \rightarrow 0$ . In general  $Q_0^2$ ,  $Q_1^2$  and  $Q_2^2$  can be slightly different. In the following section we shall consider different options.

<sup>1</sup> Please note different normalization of  $\gamma$ 's in comparison to [7].

At large Bjorken  $x$  one has to include also the so-called target mass corrections. Their origin is mainly kinematic [10]. In our approximate treatment we substitute the Bjorken variable  $x$  in the partonic distributions by the Nachtmann variable  $\xi$  [11] given by:

$$\xi = \frac{2x}{1 + \sqrt{1 + \frac{4M_N^2 x^2}{Q^2}}}, \quad (7)$$

which is the dominant modification.

In principle  $F_2^{asympt}(x, Q^2)$  could be obtained in any realistic model of the nucleon combined with QCD evolution. We leave the rather difficult problem of modeling the partonic distributions for future studies. We expect that at not too small  $x > 0.01$ , the region of the interest of the present paper, the leading order Glück-Reya-Vogt (GRV) parametrization of  $F_2^{p,asympt}(x, Q^2)$  and  $F_2^{n,asympt}(x, Q^2)$  should be adequate. Furthermore in our opinion the parametrization [9] with the valence-like input for the sea quark distributions and  $\bar{d} - \bar{u}$  asymmetry built in incorporates in a phenomenological way nonperturbative effects caused by the meson cloud in the nucleon [12].

The total cross section for (vector meson) – (nucleon) collision is not well known. Above meson-nucleon resonances, one may expect the following approximation to hold:

$$\begin{aligned} \sigma_{\rho N}^{tot} &= \sigma_{\omega N}^{tot} = \frac{1}{2} \left[ \sigma_{\pi^+ p}^{tot} + \sigma_{\pi^- p}^{tot} \right], \\ \sigma_{\phi N}^{tot} &= \sigma_{K^+ p}^{tot} + \sigma_{K^- p}^{tot} - \frac{1}{2} \left[ \sigma_{\pi^+ p}^{tot} + \sigma_{\pi^- p}^{tot} \right]. \end{aligned} \quad (8)$$

Using a simple Regge-inspired parametrizations by Donnachie-Landshoff [13] of the total  $\pi N$  and  $KN$  cross sections we get simple and economic parametrizations for energies above nucleon resonances

$$\begin{aligned} \sigma_{\rho N}^{tot} &= \sigma_{\omega N}^{tot} = 13.63 \cdot s^{0.0808} + 31.79 \cdot s^{-0.4525}, \\ \sigma_{\phi N}^{tot} &= 10.01 \cdot s^{0.0808} + 2.72 \cdot s^{-0.4525}, \end{aligned} \quad (9)$$

where the resulting cross sections are in mb.

We expect that our model should be valid in a broad range of  $x$  and  $Q^2$  except for very small  $x < 0.001$ , where genuine effects of BFKL pomeron physics could show up, and except for very large  $x$ , where the energy ( $s^{1/2}$  in (4)) is small and the behaviour of the total  $VN$  cross section is essentially unknown. Because our main interest is in the transition region, the large  $Q^2$  data were not taken into account in the fit. There the partonic contribution is by far dominant and the GRV parametrization [9] is known to provide a reliable description of the data.

### 3 Comparison to experimental data

Most of the previous parametrizations in the literature centered on the proton structure function. In the present analysis we are equally interested in both proton and neutron structure functions. Achieving this goal requires special selection of the experimental data with similar statistics and similar range in  $(x, Q^2)$  for proton and deuteron

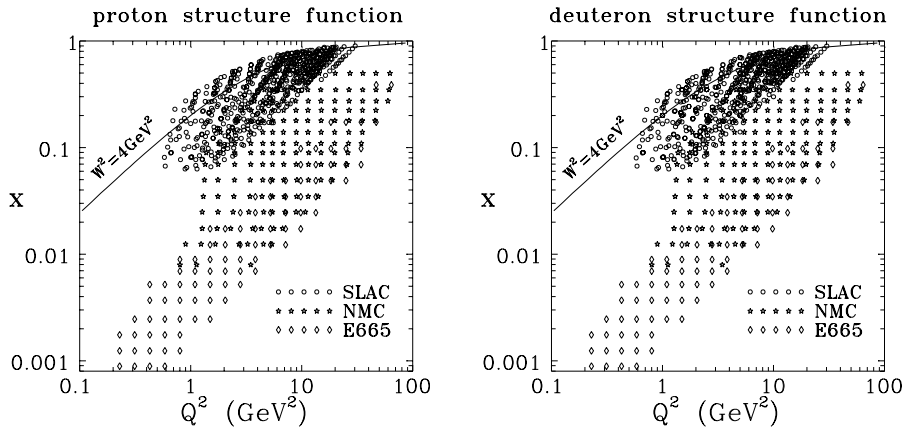


**Fig. 1.** The presentation in the  $(x, Q^2)$  plane of the experimental data included in the fit for proton (left panel) and deuteron (right panel) structure functions. For reference shown are lines with constant  $W = 2$  GeV which conventionally separate resonance and DIS regions

structure function. In Fig. 1 we display the experimental data for proton (left panel) and deuteron (right panel) structure functions chosen in our fit. We have selected only NMC, E665 and SLAC sets of data [18] for both proton and deuteron structure functions, together amounting to 1833 experimental points: 901 for the proton structure function and 932 for the deuteron structure function. According to the arguments presented above, we have omitted BCDMS and HERA data in the fitting procedure but these will be compared to our parametrization when discussing the quality of the fit.

The deuteron structure function has been calculated as

$$F_2^d(x, Q^2) = \frac{1}{2}[F_2^p(x, Q^2) + F_2^n(x, Q^2)], \quad (10)$$

i.e. we have neglected all nuclear effects such as shadowing, antishadowing due to excess mesons, Fermi motion, binding, etc, which are known to be relatively small for the structure function of the deuteron [14–16], one of the most loosely bound nuclear systems. In addition we have assumed isospin symmetry for the proton and neutron quark distributions, i.e.  $u_n(x, Q^2) = d_p(x, Q^2)$ ,  $d_n(x, Q^2) = u_p(x, Q^2)$  and  $s_n(x, Q^2) = s_p(x, Q^2)$ . The charm contribution, which in the GRV parametrization [9] is due to the photon-gluon fusion, is in practice negligible in the region of  $x$  and  $Q^2$  taken in the fit, and therefore is omitted throughout the present analysis.

The results of the fit are summarised in Table 1. Because in general  $Q_0^2$ ,  $Q_1^2$  and  $Q_2^2$  can be different, there are 4 independent free parameters of the model. In order to limit the number of parameters we have imposed extra conditions as specified in Table 1. A series of seven fits has been performed. In all cases considered the number of free parameters has been reduced to two: the cut-off parameter of the form factor and  $Q_0^2$ . Statistical and systematic errors were added in quadrature when calculating  $\chi^2$ . Only data with  $Q^2 > 0.25$  GeV<sup>2</sup> were taken in the fit which is connected with the domain of applicability of the GRV parametrization. The values of the parameters found are given in each case in parentheses below the value of  $\chi^2$  per degree of freedom. In addition to the combined fit, which includes both proton  $F_2^p$  and deuteron  $F_2^d$  structure function data, we show the result of the fit sep-

arately for proton and deuteron structure functions. As can be seen from the table fairly similar values of parameters are found for the proton and deuteron structure function and the  $\chi^2$  per degree of freedom is slightly worse in the latter case which can be due to the omission of nuclear effects as mentioned above. The best fit (No 1 in the table) is obtained with  $Q_1^2 = Q_2^2 = 0$  (fits of similar quality can be obtained with very small values of  $Q_1^2 \sim 0.1$  GeV<sup>2</sup> and  $Q_2^2 \sim 0.1$  GeV<sup>2</sup>). While the value of  $\chi^2$  does not practically depend on the type of the form factor (exponential vs. Gaussian), much larger value of  $Q_0^2$  is found for the Gaussian ( $Q_0^2 = 0.84$  GeV<sup>2</sup>) than for the exponential ( $Q_0^2 = 0.52$  GeV<sup>2</sup>) parametrization. The value of  $Q_0^2$  found here is smaller than in the original Badełek-Kwieciński model [7] but larger than that found by H1 collaboration in the fit to low- $x$  data [3].

Although the resulting  $\chi^2$  is similar in both cases, the  $F_2^n(x)/F_2^p(x)$  ratio for  $x \rightarrow 1$  prefers the Gaussian form factor. While the vector meson contribution with the exponential form factor survives up to relatively large  $x$ , with the Gaussian form factor it is negligible at large  $x$ .

For comparison the GRV parametrization of quark distributions alone yields:

$$\begin{aligned} \chi^2/N_{dof} &= 9.74 \text{ (21.48)} \text{ (proton structure functions),} \\ \chi^2/N_{dof} &= 13.73 \text{ (32.99)} \text{ (deuteron structure functions),} \\ \chi^2/N_{dof} &= 11.77 \text{ (27.33)} \text{ (combined data),} \end{aligned}$$

where the first numbers include target mass corrections and for illustration in parentheses their counterparts without target mass corrections are given. Clearly the inclusion of the target mass effects is essential and only such results will be discussed in the course of the present paper.

The agreement of the CKMT parametrization is comparable to that obtained in our model. For instance for parametrization (b) in Table 2 in the second paper [6], which includes new HERA data:

$$\begin{aligned} \chi^2/N_{dof} &= 2.22 \text{ (1.00)} \text{ (proton structure functions),} \\ \chi^2/N_{dof} &= 3.54 \text{ (3.59)} \text{ (deuteron structure functions),} \\ \chi^2/N_{dof} &= 2.89 \text{ (2.33)} \text{ (combined data),} \end{aligned}$$

where in the parentheses we present  $\chi^2$  for  $Q^2 < 4$  GeV<sup>2</sup> i.e. in the region of applicability of the CKMT parametriza-

**Table 1.** A compilation of the results obtained from our fit. The  $\chi^2$  per degree of freedom are given in first lines whereas the pairs of numbers in second lines are the parameters ( $\lambda$  (GeV),  $Q_0^2$  (GeV<sup>2</sup>)) found in the fit

case	exponential			Gaussian		
	$F_2^p$ and $F_2^d$	$F_2^p$	$F_2^d$	$F_2^p$ and $F_2^d$	$F_2^p$	$F_2^d$
1) $Q_1^2 = Q_2^2 = 0$	2.39 (0.31,0.52)	2.13 (0.30,0.51)	2.63 (0.31,0.53)	2.38 (0.50,0.84)	1.90 (0.49,0.77)	2.66 (0.50,0.87)
2a) $Q_1^2 = Q_0^2$	3.24 (0.34,0.51)	2.79 (0.33,0.50)	3.68 (0.34,0.51)	2.79 (0.53,0.77)	2.27 (0.53,0.77)	3.15 (0.53,0.84)
2b) $Q_1^2 = 0.5$ GeV <sup>2</sup>	3.20 (0.34,0.53)	2.77 (0.34,0.52)	3.61 (0.34,0.53)	2.53 (0.52,0.82)	2.05 (0.52,0.78)	2.85 (0.52,0.85)
3a) $Q_2^2 = Q_0^2$	4.13 (0.37,0.43)	3.46 (0.36,0.44)	4.74 (0.37,0.43)	3.60 (0.56,0.66)	3.14 (0.57,0.66)	4.02 (0.56,0.66)
3b) $Q_2^2 = 0.5$ GeV <sup>2</sup>	4.50 (0.40,0.47)	3.67 (0.39,0.48)	5.24 (0.39,0.45)	2.88 (0.56,0.73)	2.48 (0.56,0.72)	3.24 (0.55,0.74)
4a) $Q_1^2 = Q_2^2 = Q_0^2$	5.92 (0.38,0.40)	4.96 (0.38,0.41)	6.79 (0.38,0.38)	5.49 (0.58,0.60)	4.74 (0.58,0.60)	6.20 (0.57,0.60)
4b) $Q_1^2 = Q_2^2 = 0.5$ GeV <sup>2</sup>	7.06 (0.43,0.45)	5.67 (0.43,0.47)	8.32 (0.42,0.43)	4.26 (0.57,0.70)	3.63 (0.58,0.70)	4.84 (0.57,0.70)

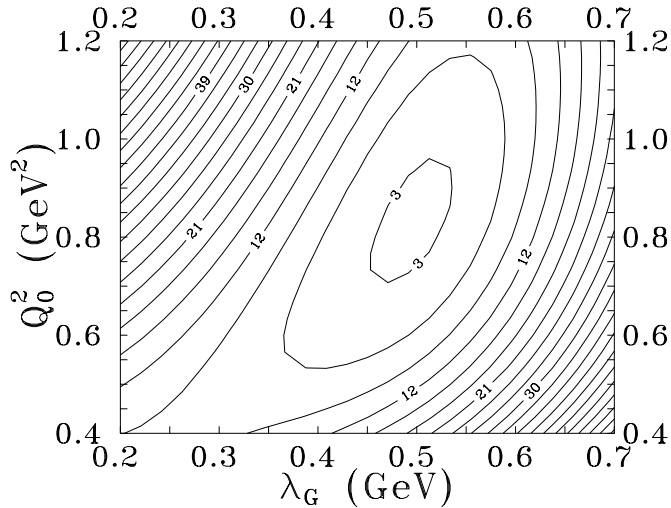


**Fig. 2.** A map of the  $\chi^2$  per degree of freedom in the  $(\lambda, Q_0^2)$  space of the model parameters for combined fit to the proton and deuteron structure functions with the Gaussian form factor

tion.<sup>2</sup> We note much better description of the proton data in comparison to the deuteron data. The agreement of the Donnachie-Landshoff parametrization [5] with the proton structure function data is of similar quality.

In Fig. 2 we present for completeness a map of  $\chi^2$  for our best fit as a function of model parameters  $Q_0^2$  and  $\lambda$ . A well defined minimum of  $\chi^2$  for  $\lambda_G \approx 0.5$  GeV and  $Q_0^2 \approx 0.85$  GeV<sup>2</sup> can be seen. The experimental statistical

uncertainty of the obtained parameters  $\lambda_G$  and  $Q_0^2$  is less than 1 %.

Some examples of the fit quality can be seen in Fig. 3 ( $x$ -dependence for different values of  $Q^2 = 0.585, 1.1, 2.0, 3.5$  GeV<sup>2</sup>) and in Figs. 4, 5 ( $Q^2$ -dependence for different values of Bjorken  $x = 0.00127, 0.0125, 0.05, 0.10, 0.18, 0.35, 0.55, 0.75$ ). Shown are experimental data [18] which differ from the nominal  $Q^2$  or Bjorken  $x$  specified in Fig. 3, 4, 5 by less than  $\pm 3$  %. An excellent fit is obtained for  $Q^2 > 4$  GeV<sup>2</sup> (not shown in Fig. 3), although the VDM contribution stays large up to 10 GeV<sup>2</sup>. In comparison to the GRV parametrization (dashed line) our model describes much better the region of small  $Q^2 < 3$  GeV<sup>2</sup>, especially at intermediate Bjorken  $x$ :  $0.05 < x < 0.4$ . The CKMT model (long-dashed line), shown according to the philosophy in [6] for  $Q^2 < 10$  GeV<sup>2</sup> gives a better fit at very small Bjorken  $x$ . However, one may expect here a few more effects which will be discussed below.<sup>3</sup> It is however slightly worse as far as isovector quantities are considered, as will be discussed later. There seems to be a systematically small (up to about 5 %) discrepancy between our model and the data for  $Q^2 < 2$  GeV<sup>2</sup> and  $x = 0.1 - 0.3$ . This is caused by some higher-twist effects due to the production of the  $\pi N$  [17] and  $\pi\Delta$  exclusive channels and will be discussed elsewhere. A fit of similar quality is obtained in our model for the proton (left panels) and deuteron (right panels) structure functions. Rather good agreement of our model with the BCDMS data can be observed in Figs. 4 and 5 in spite of the fact that the data were not used in the fitting procedure.

<sup>2</sup> The number of experimental points is reduced then to 354 and 373 for proton and deuteron structure functions, respectively

<sup>3</sup> The use of the next-to-leading order structure functions [9] in our model would improve the description of low- $x$  data, discussion of which is left for a separate analysis.

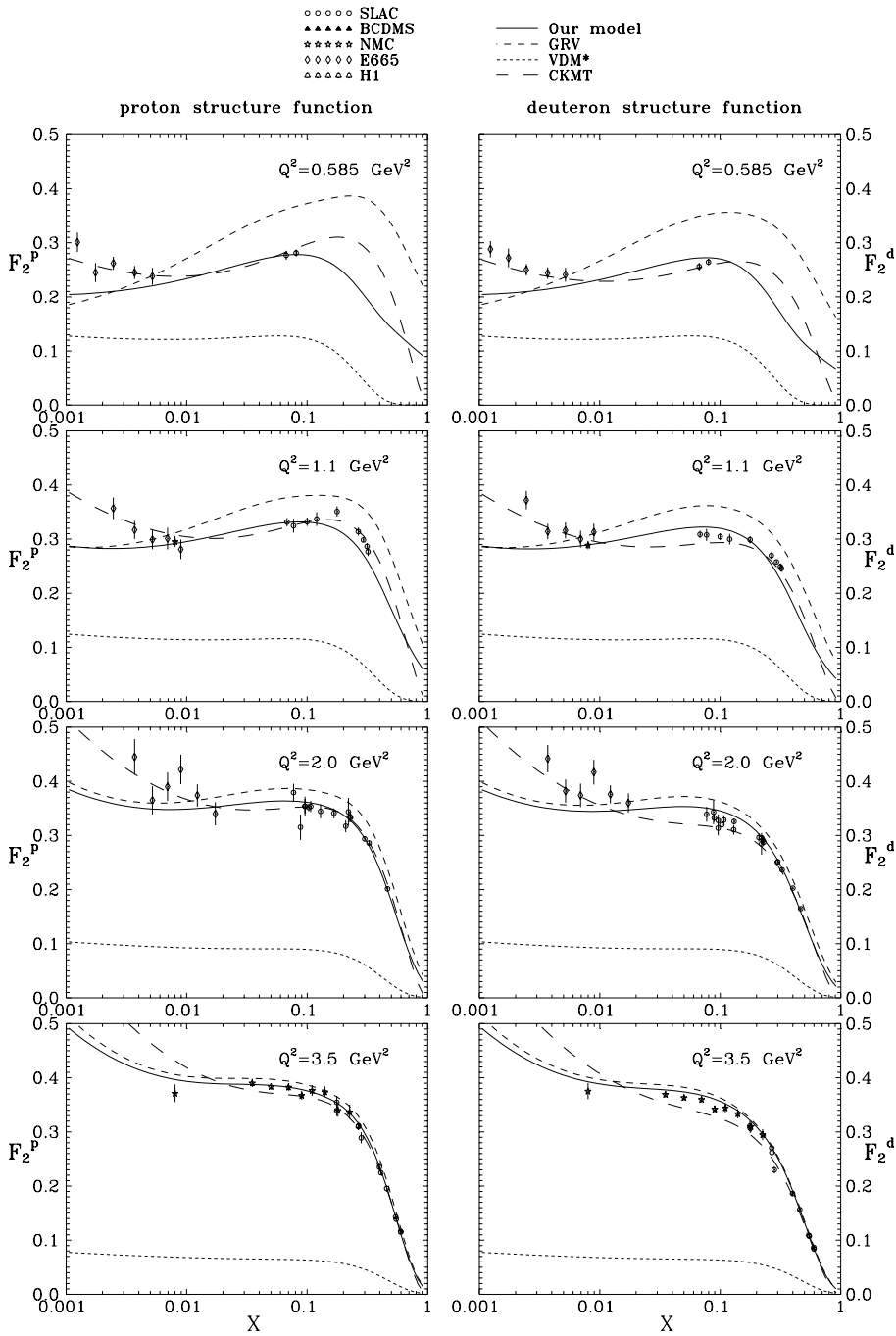


**Fig. 3.** Comparison of the model results with experimental data for  $F_2^p$  (l.h.s) and  $F_2^d$  (r.h.s.) as a function of Bjorken  $x$  for different values of  $Q^2 = 0.585, 1.1, 2.0, 3.5 \text{ GeV}^2$ . The solid line corresponds to our full model with the Gaussian form factor. We present also the modified VDM contribution (short-dashed) and for comparison also the result obtained with GRV parametrization [9] (corrected for target mass effects) of quark distributions (dashed line) and that of the CKMT model [6] (long-dashed line)

At very small  $x < 0.01$  the description of the data becomes worse. This is partially due to the use of the leading order approximation. The fit to the fixed-target data prefers  $\bar{x} \approx x$  and  $\bar{Q}^2 \approx Q^2$  (see Table 1 and the discussion therein). On the other hand, the HERA data would prefer  $Q_1^2 \neq 0$  and  $Q_2^2 \neq 0$ . If we included the HERA data in the fit the description of the fixed target data would become worse. There are no fundamental reasons for the parameters in both regions to be identical. In addition at very small  $x$  other effects of isoscalar character, not included here, such as heavy long-lived fluctuations of the

incoming photon [19] and/or BFKL pomeron effects [20], may become important.

For illustration a VDM contribution modified by a form factor (5) is shown separately by the short-dashed line. The partonic component can be obtained as a difference between the solid and VDM line. It can be seen from Figs. 3-5 that the partonic component decreases towards small  $Q^2$ . This decrease is faster than one could directly infer from the failure of the GRV parametrization at low  $Q^2$  because in our model a part of the strength resides in the VDM contribution. The modified VDM contribution is sizeable for small values of Bjorken  $x$  and not too large  $Q^2$

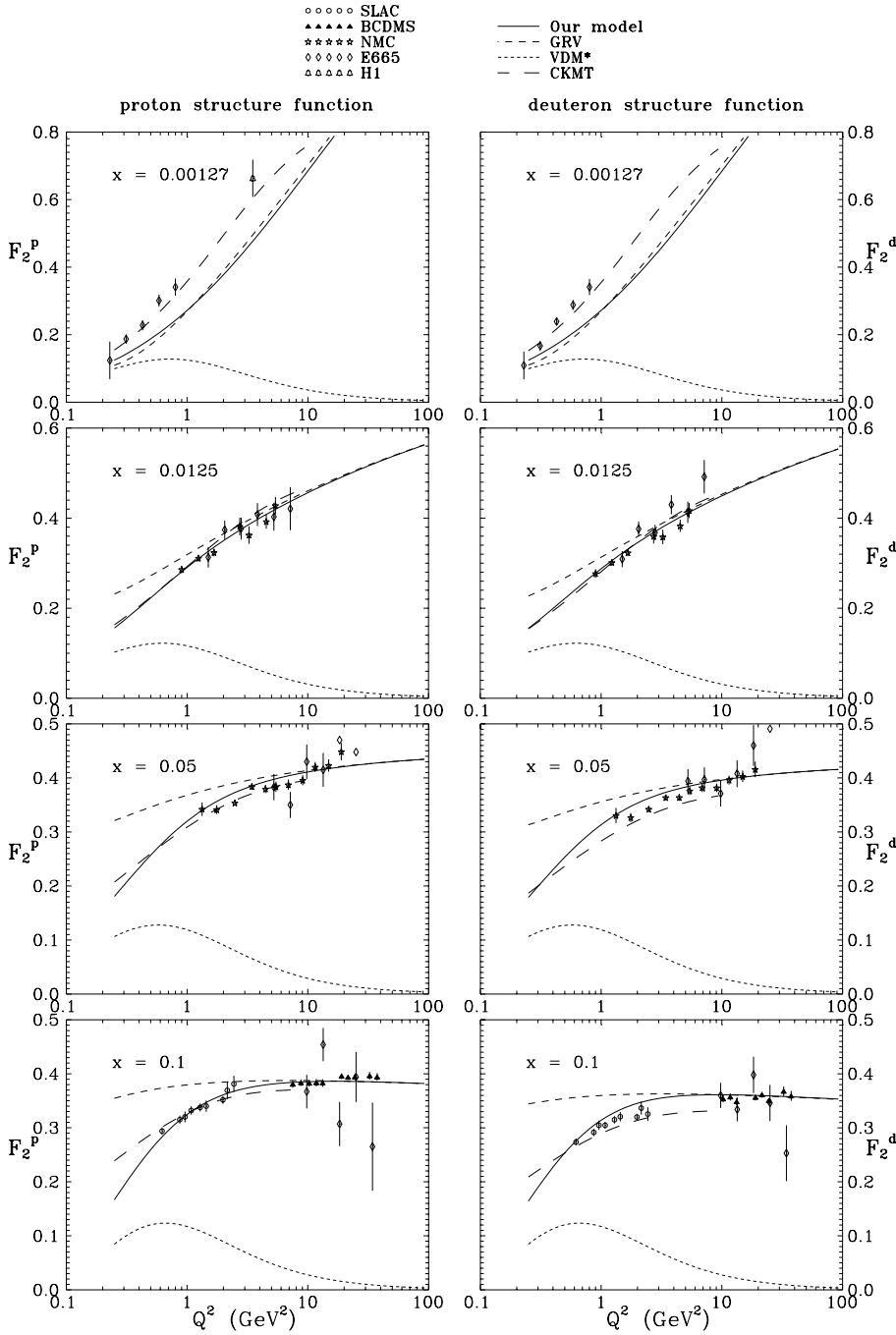


**Fig. 4.** The same as in Fig. 3 as a function of  $Q^2$  for different values of  $x = 0.00127, 0.0125, 0.05, 0.10$

and survives up to relatively large  $Q^2$ . At  $Q^2 > 3.5 \text{ GeV}^2$  the structure functions in our model almost coincide with those in the GRV parametrization despite that the VDM term is still not small. For  $Q^2 \rightarrow \infty$  only the partonic contribution survives and  $F_2(x, Q^2) \rightarrow F_2^{part}(x, Q^2) \rightarrow F_2^{GRV}(x, Q^2)$ .

The deviations from the partonic model can be also studied in the language of higher-twist corrections. Then the structure function can be written formally as

$$F_2^{p/n}(x, Q^2) = F_2^{p/n,LT}(x, Q^2)$$

$$\times \left[ 1 + \frac{c_2^{p/n}(x)}{Q^2} + \frac{c_4^{p/n}(x)}{Q^4} + \dots \right]. \quad (11)$$

However, in empirical analyses one usually includes only one term in (11)

$$F_2^{p/n}(x, Q^2) = F_2^{p/n,LT}(x, Q^2) \left[ 1 + \frac{c^{p/n}(x)}{Q^2} \right]. \quad (12)$$

In our model for  $Q^2 \sim M_V^2, Q_0^2$  there are an infinite number of active terms in the expansion of the structure function (11). Therefore the coefficient  $c^{p/n}$  (the same is true for the deuteron counterpart  $c^d$ ) in (12) becomes effectively  $Q^2$ -dependent  $c^{p/n}(x) = c^{p/n}(x, Q^2)$ .

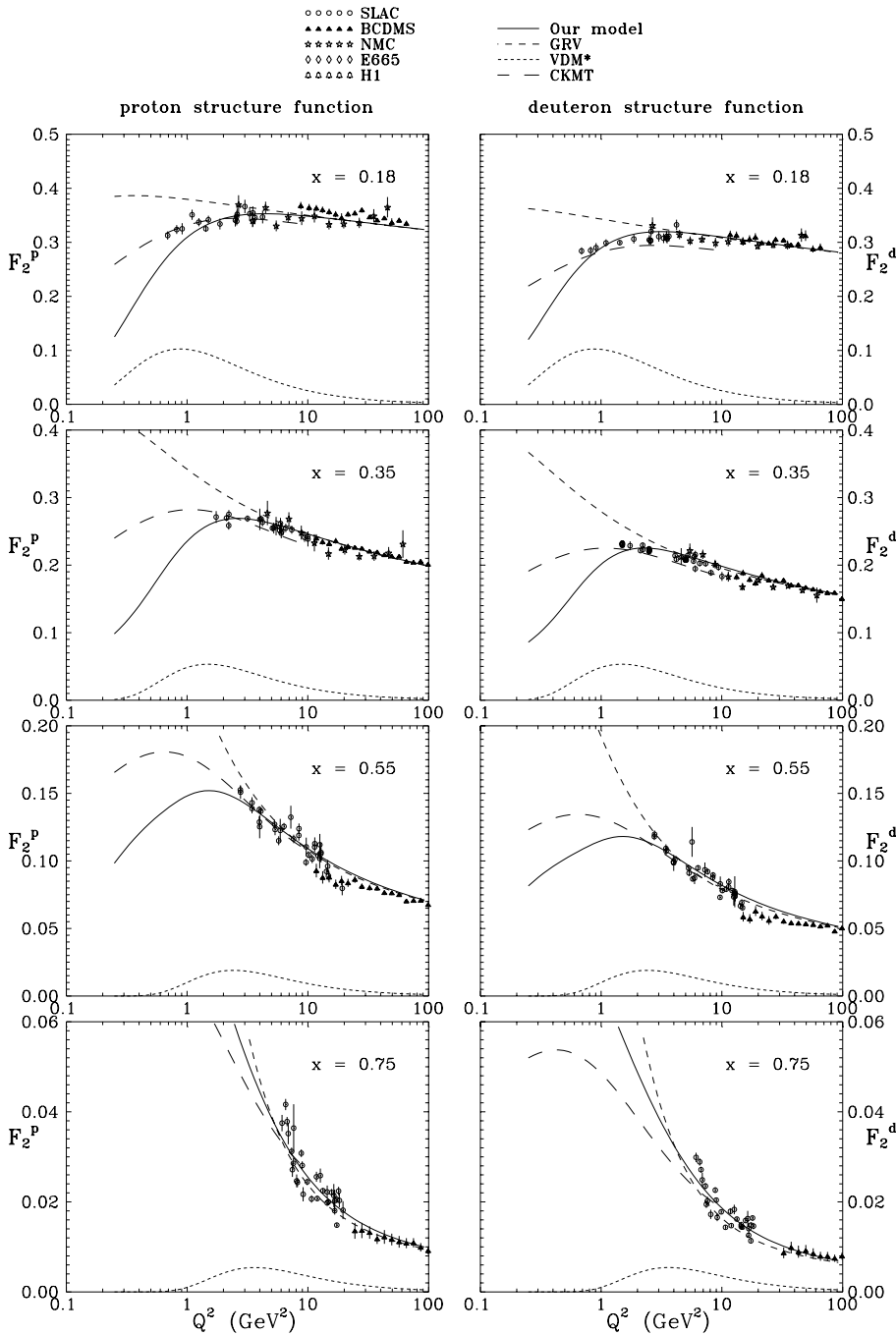


**Fig. 5.** The same as in Fig. 4 for different values of  $x = 0.18, 0.35, 0.55, 0.75$

As an example in Fig. 6 we show  $c^p$  and  $c^d$  as a function of Bjorken  $x$  for three different values of  $Q^2 = 2, 4, 8 \text{ GeV}^2$  in the range relevant for the analysis in [23]. In order to correctly compare our results for  $c^p$  and  $c^d$  with the results of the analysis in [23] the structure function  $F_2^{p/n,LT}(x, Q^2)$  in (12) will include complete target mass corrections calculated according to [10]. A fairly similar pattern is obtained for  $c^p$  and  $c^d$  especially at small  $x$ . The rise of  $c^p$  or  $c^d$  for  $x \rightarrow 1$  is caused by our treatment of the target mass corrections and partially by the VDM contribution which survives in our model up to relatively large  $x$ . We obtain small negative  $c^p$  and  $c^d$  for  $x < 0.3$

in agreement with [23]. The smallest of  $c^p$  and  $c^d$  in our model for  $x < 0.3$  is due to the cancellation of the positive VDM contribution and a negative contribution caused by the external damping factor  $\frac{Q^2}{Q^2 + Q_0^2}$  of the partonic contribution in (6). The CKMT parametrization [6] (shown only in its applicability range for  $Q^2 = 2, 4 \text{ GeV}^2$ ) provides a very good explanation of  $c^p$ . It predicts, however, somewhat larger negative  $c^d$  for  $x < 0.3$ . This will have some unwanted consequences for  $c^p - c^n$  discussed below.

In Fig. 7 we show  $c^p - c^n$  for  $Q^2 = 2, 4 \text{ GeV}^2$  together with empirical results from [24]. Rather strong  $Q^2$ -dependence of  $c^p - c^n$  is observed. Our model correctly de-

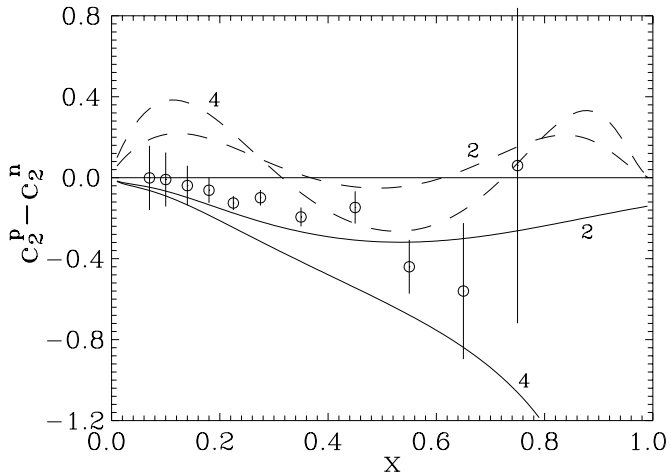


**Fig. 7.** The difference of twist-four coefficients  $c^p - c^n$ . The data points are from [24]. The solid lines are the results of our model while the dashed lines are obtained with the CKMT-parametrization. In both cases the two curves are for  $Q^2 = 2, 4$  GeV<sup>2</sup>

describes the trend of the experimental data. For comparison we show also the result obtained by means of the CKMT parametrization (long-dashed lines) of the structure functions which somewhat fails to reproduce the details of the empirical results from [24], especially for small Bjorken  $x$ . To our best knowledge no other model in the literature is able to describe quantitatively this subtle higher-twist effect.

Our model seems to provide a very good description of some isovector quantities. As an example in Fig. 8 we present  $F_2^p(x, Q^2) - F_2^n(x, Q^2)$  at  $Q^2 = 4$  GeV<sup>2</sup> obtained in our model (solid lines for different form factors), as well as the results obtained with the GRV parametrization (dashed line) and in the CKMT model (long-dashed line).<sup>4</sup> The NMC data [21] prefer rather our model. As a consequence of the imperfect description of the deuteron data the CKMT model fails to describe the difference  $F_2^p(x) - F_2^n(x)$  for  $x < 0.3$ . The success of our model is related to the violation of the Gottfried Sum Rule and/or  $\bar{d} - \bar{u}$  asymmetry which is included in our model explicitly. In contrast to our model in the CKMT model for  $Q^2 > 2$  GeV<sup>2</sup> the Gottfried Sum Rule  $S_G = \frac{1}{3}$ .

## 4 Conclusions and discussion

We have constructed a simple model incorporating non-perturbative structure of the nucleon and photon. Our model is a generalization of the well known and successful Badelek-Kwieciński model [7]. While the original Badelek-Kwieciński model is by construction limited to a small- $x$  region, our model is intended to be valid in much broader range. The original VDM model assumes implicitly a large

<sup>4</sup> No evolution of the CKMT quark distributions was done, but it is negligible between  $2 \rightarrow 4$  GeV<sup>2</sup> for the nonsinglet quantity.

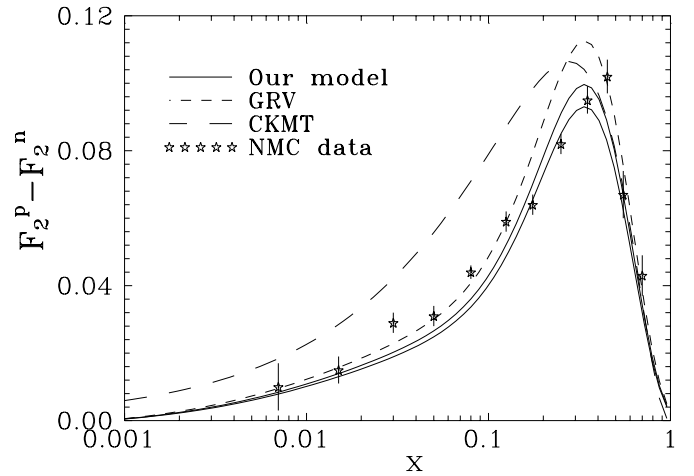


**Fig. 8.**  $F_2^p(x, Q^2) - F_2^n(x, Q^2)$  at  $Q^2 = 4$  GeV<sup>2</sup> compared to the NMC data. The upper solid line corresponds to our model with the exponential form factor, the lower solid line to our model with the Gaussian form factor, the dashed line to the GRV parametrization and the long-dashed line to the CKMT parametrization

coherence length for the photon-hadron fluctuation, i.e. assumes that the hadronic fluctuation is formed far upstream of the target. When the fluctuation length becomes small the VDM is expected to break-down. This effect has been modelled by introducing an extra form factor. As a result we have succeeded in constructing a physically motivated parametrization of both proton and deuteron structure functions. In comparison to the pure partonic models with QCD evolution our model leads to a much better agreement at low  $Q^2$  in a broad range of  $x$ .

With only two free parameters we have managed to describe well the transition from the high- to low- $Q^2$  region simultaneously for the proton and deuteron structure functions. Our analysis of the experimental data indicates that the QCD parton model begins to fail already at  $Q^2$  as high as about 3 GeV<sup>2</sup>. This value is larger than commonly believed.

In our discussion we have omitted the region of the HERA data. In our opinion the physics there may be slightly more complicated. Other effects of isoscalar character, not included in our analysis, for example the BFKL pomeron effects [20], may become important.

In contrast to other models in the literature we obtain a very good description of the NMC  $F_2^p - F_2^n$  data [21] where the previously mentioned isoscalar effects cancel.

Recently an intriguing, although small, difference between  $\bar{d} - \bar{u}$  asymmetry obtained from recent E866 Drell-Yan data [22] and muon DIS NMC data [21] has been observed. At least part of the difference can be understood in our model. We expect for  $Q^2$  smaller than about 4 GeV<sup>2</sup> an extra  $Q^2$  dependence of some parton model sum rules. We predict a rather strong  $Q^2$  effect for the integrand of the Gottfried Sum Rule where in the first approximation the VDM contribution cancels.

Recently in the literature there has been sizeable activity towards a better understanding of higher-twist effects.



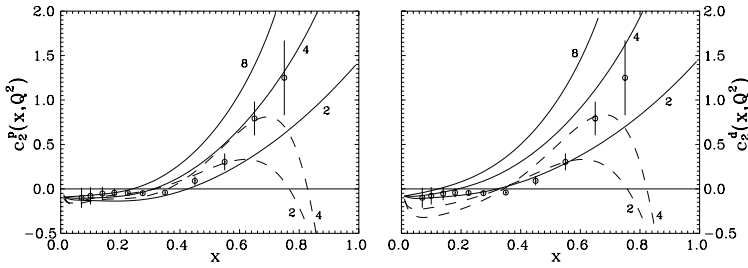


**Fig. 6.** The twist-four coefficients  $c^p$  and  $c^d$  defined by (12) obtained in our model for  $Q^2 = 2, 4, 8 \text{ GeV}^2$ . The coefficients obtained from the CKMT parametrization are shown by the long-dashed line for  $Q^2 = 2, 4 \text{ GeV}^2$ . The experimental data are taken from [23]

Some were estimated within the operator product expansion, some in terms of the QCD sum rules. It is, however, rather difficult to predict the absolute normalization of the higher-twist effects. Our model leads to relatively large higher-twist contributions. For some observables, like structure functions, they almost cancel. For other observables, like  $F_2^p - F_2^n$ , the cancellation is not so effective. Our model provides specific higher-twist effects not discussed to date in the literature. This will be a subject of a future separate analysis.

*Acknowledgements.* We are especially indebted to J. Kwieciński for valuable discussions and suggestions and J. Outhwaite for careful reading of the manuscript. We would also like to thank C. Merino for the discussion of the details of the CKMT model. This work was supported partly by the German-Polish exchange program, grant No. POL-81-97.

## References

1. B. Badelek, J. Kwieciński, *Rev. Mod. Phys.* **68** (1996) 445
2. A.D. Martin, W.J. Stirling, R.G. Roberts, *Phys. Rev. D* **51** (1995) 4756
3. H1 collaboration, *Nucl. Phys. B* **470** (1997) 3; *Nucl. Phys. B* **497** (1997) 3
4. ZEUS collaboration, *Z. Phys. C* **69** (1996) 607; *Phys. Lett. B* **407** (1997) 432
5. A. Donnachie, P.V. Landshoff, *Z. Phys. C* **61** (1994) 139
6. A. Capella, A. Kaidalov, C. Merino, J. Tran Thanh Van, *Phys. Lett. B* **337** (1994) 358; A.B. Kaidalov, C. Merino, hep-ph/9806367
7. J. Kwieciński, B. Badelek, *Z. Phys. C* **43** (1989) 251; B. Badelek, J. Kwieciński, *Phys. Lett. B* **295** (1992) 263
8. B.L. Ioffe, V.A. Khoze, L.N. Lipatov, *Hard Processes; Phenomenology, Quark-Parton Model*, North Holland, Amsterdam 1984
9. M. Glück, E. Reya, A. Vogt, *Z. Phys. C* **67** (1995) 433
10. H. Georgi, H.D. Politzer, *Phys. Rev.* **14** (1976) 1829
11. O. Nachtmann, *Nucl. Phys.* **63** (1973) 237; **78** (1974) 455
12. H. Holtmann, A. Szczurek, J. Speth, *Nucl. Phys. A* **569** (1996) 631; A. Szczurek, M. Ericson, H. Holtmann, J. Speth, *Nucl. Phys. A* **596** (1996) 397
13. A. Donnachie, P.V. Landshoff, *Phys. Lett. B* **296** (1992) 227
14. B. Badelek, J. Kwieciński, *Nucl. Phys. B* **370** (1992) 278
15. V.R. Zoller, *Z. Phys. C* **53** (1992) 443
16. W. Melnitchouk, A.W. Thomas, *Phys. Rev. D* **47** (1993) 3783
17. J.D. Sullivan, *Phys. Rev. D* **5** (1972) 1732
18. <http://durpdg.dur.ac.uk/HEPDATA>
19. P. Mosey, G. Shaw, *Phys. Rev. D* **52** (1995) 4941; G. Kerley, G. Shaw, hep-ph/9707465, *Phys. Rev. D* **56** (1997) 7291
20. N.N. Nikolaev, B.K. Zakharov, *Z. Phys. C* **53** (1992) 331; N.N. Nikolaev, B.K. Zakharov, *Z. Phys.* **64** (1994) 631; J. Kwieciński, A.D. Martin, A.M. Staśto, *Phys. Rev. D* **56** (1997) 3991; A.D. Martin, M.G. Ryskin, A.M. Staśto, *Eur. Phys. J. C* **7** (1999) 643, hep-ph/9806212; N.N. Nikolaev, V.R. Zoller, hep-ph/9812446
21. NMC collaboration, M. Arneodo et al., *Phys. Rev. D* **50** (1994) R1
22. E866/NuSea collaboration, E.A. Hawker et al., *Phys. Rev. Lett.* **80** (1998) 3715
23. M. Virchaux, A. Milsztajn, *Phys. Lett. B* **274** (1992) 221
24. NMC collaboration, *Nucl. Phys. B* **371** (1992) 3